Nineteenth Quarterly Progress Report

February 1, 2011 to April 30, 2011
Contract No. HHS-N-260-2006-00005-C
Neurophysiological Studies of Electrical Stimulation for the Vestibular Nerve

Submitted by:
James O. Phillips, Ph.D.[1,3,4]
Steven Bierer, Ph.D. [1,3,4]
Albert F. Fuchs, Ph.D. [2,3,4]
Justin Golub, M.D. [1]
Chris R.S. Kaneko, Ph.D. [2,3]
Leo Ling, Ph.D. [2,3]
Shawn Newlands, M.D., Ph.D. [5]
Kaibao Nie, Ph.D. [1,4]
Jay T. Rubinstein, M.D., Ph.D. [1,4,6]

[1] Department of Otolaryngology-HNS, University of Washington, Seattle, Washington
[2] Department of Physiology and Biophysics, University of Washington, Seattle, Washington
[3] Washington National Primate Research Center, University of Washington, Seattle, Washington
[4] Virginia Merrill Bloedel Hearing Research Center, University of Washington, Seattle, Washington
[5]Department of Otolaryngology, University of Rochester, Rochester, New York
[6] Department of Bioengineering, University of Washington, Seattle, Washington

Reporting Period: February 1, 2011 to April 30, 2011

Challenges:

1. During Quarter 19 we received notification from Cochlear Corporation that there were issues with the Laura 34 research interface that could potentially affect our stimulation results. This interface was used in most of our recording and stimulation experiments, and is the hardware on which our VI Stream testing software is based. The reported issue has to do with the signal level of the RF link on the research interface. This was set too low by the manufacturer and could, under certain circumstances, produce a loss or drop out of commanded biphasic stimulus pulses. This could produce an under-representation of the effects of the commanded stimulation.

Our response to this challenge was to reexamine the data that we obtained with the Laura 34 interface. We have a significant advantage over many research protocols in that we record a stimulation artifact either with surface electrodes or with tungsten microelectrodes during electrical stimulation for both behavioral studies and unit recording studies. Indeed, we play the stimulation artifact through the loudspeaker in the laboratory and display it in real time, so that we can hear and see the stimulation as it occurs. The result of this procedure is that we are confident that none of our analyzed data was contaminated with this artifact. However, it is important to note that recording in one animal was stopped and the animal was sacrificed after the stimulus train became erratic at higher frequency stimulation rates. This animal had been implanted many months earlier and was used for behavioral and unit recording experiments for a year while the implant performed correctly. During this time the animal had grown considerably, and the amount of overlying tissue at the RF link had increased. We attributed this loss of implant function to a chamber infection that, we thought at the time, might have compromised the integrity of the vestibular implant electrode array. There was no evidence of this at necropsy. We now suspect that it is possible that the implant was in fact functioning properly, and the inconsistent stimulation that we encountered was the result of the recently identified issue with the Laura 34. If this is the case, then we have in-vivo recording of the development of a Laura 34 failure mode in a primate model, which might be useful to Cochlear Corporation or other researchers as they address this issue.

Successes: We have made important progress in several areas as noted below.

1. We have continued our brainstem recording experiments with the objective of determining if downstream brainstem neurons that are responsible for the generation of nystagmus are activated in a physiologically normal pattern by electrical stimulation. In addition to recording from vestibular nucleus neurons, we recorded from burst and omnipause neurons in the paramedian pontine reticular formation (PPRF) during electrical stimulation. Figure 1 shows the activity of an omnipause neuron (OPN) recorded 2 mm rostral to the abducens nucleus in a monkey. This neuron can be identified by its location adjacent to the rootlets of the abducens

nerve, which display a characteristic burst tonic discharge. The omnipause neurons discharge tonically during visual fixation or gaze holding, and pause for vestibular fast phases, blinks, and saccadic eye movements in all directions. The neuron discharge in Figure 1A shows this characteristic activity during spontaneous saccades in the dark. The neuron pauses for each saccadic eye movement, and discharges at a sustained rate during fixation. In Figure 1B, during constant frequency and constant current electrical stimulation of the right lateral canal with a train of biphasic pulses, the animal displays a right beating constant velocity nystagmus. Again, the neuron discharges at a sustained rate during the slow phase of nystagmus, and again it pauses for each fast phase eye movement and saccade. Qualitatively, the responses are similar. However, closer inspection suggests that the response during electrical stimulation is not identical to that during natural saccades. Note that the duration of the pause for saccades in Figure 1A (red vertical lines) closely matches the duration of the saccadic eye movement. However, in Figure 1B, the duration of the pause (red vertical lines) often significantly outlasts the duration of the fast phase eye movement. The tight control of fast phase duration by omnipause neuron activity is actually compromised by the electrical stimulation.

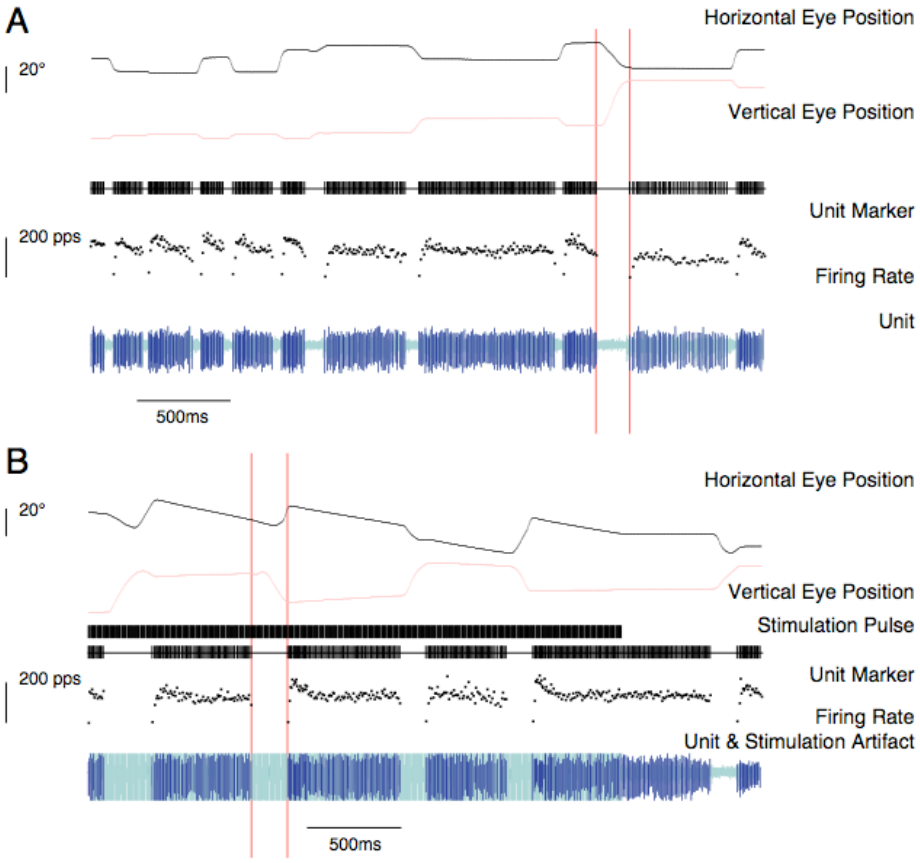

Figure 1: Omnipause neuron activity during saccadic eye movements and electrically elicited nystagmus. A) Neuron activity recorded during spontaneous saccades in the dark. B) Neuron activity recorded during nystagmus elicited by electrical stimulation.

A similar relationship between rapid eye movement and neuron discharge is also displayed by short lead burst neurons in the PPRF. Figure 2 displays the activity of a

presumed short lead excitatory burst neuron (EBN) recorded rostral of the abducens nucleus. Such neurons are thought to be inhibited by omnipause neurons, and to make direct excitatory synaptic connections with abducens motoneurons. They burst primarily during ipsilaterally directed saccadic eye movements and vestibular fast phases. They provide the burst discharge in motoneurons that drive such high velocity horizontal eye movements.

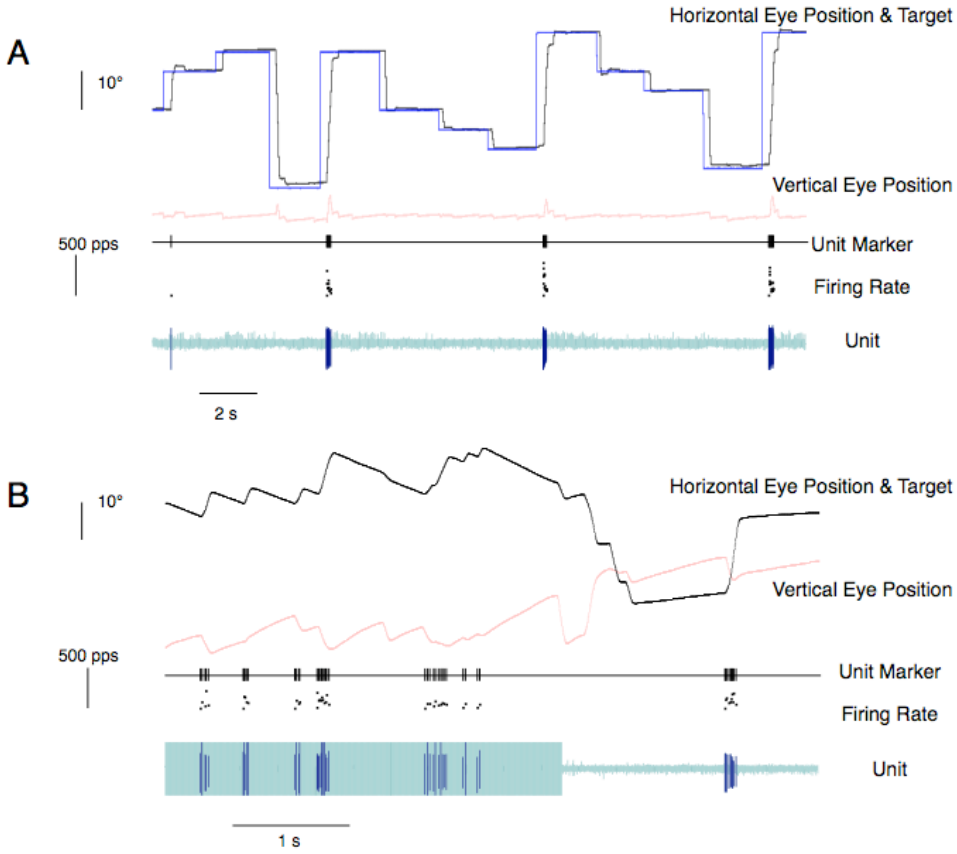

Figure 2. Excitatory burst neuron discharge during saccadic eye movements and electrically elicited nystagmus. A) Neuron activity recorded during saccades to stepped visual targets. B) Neuron activity recorded during nystagmus elicited by electrical stimulation.

In Figure 2A an EBN recorded in the right PPRF displays a burst discharge during each saccade to the right. In Figure 2B, which is displayed at a higher temporal resolution, the same neuron discharges for each fast phase eye movement during the electrical stimulation, and for a rightward spontaneous saccade in the dark after the end of electrical stimulation. In this case, the relationships between the burst discharge and the rapid eye movement are not as easy to see as they were in Figure 1. Therefore, in Figure 3, we plotted the quantitative relationship between burst duration and saccade or fast phase duration, and the relationship between the number of spikes in the burst and saccade or fast phase amplitude. Figure 3A shows that while the duration of the burst is shorter than the duration of either visually elicited saccades (open blue circles) or electrically elicited slow phases (filled red squares), burst duration for a given rapid eye

movement amplitude is typically longer for electrically elicited movements than for visually elicited movements; i.e., the filled red squares are shifted up from the open blue circles. Figure 3B shows that the number of spikes in the burst is greater for electrically elicited slow phases (red filled circles) than for comparably sized visually elicited saccades (open blue squares); i.e., the filled red circles are shifted up from the open blue squares. Clearly, these preliminary observations suggest that the quantitative relationships between the burst neuron discharge and the observed movement change depending on whether the movement is elicited by electrical or visual stimuli.

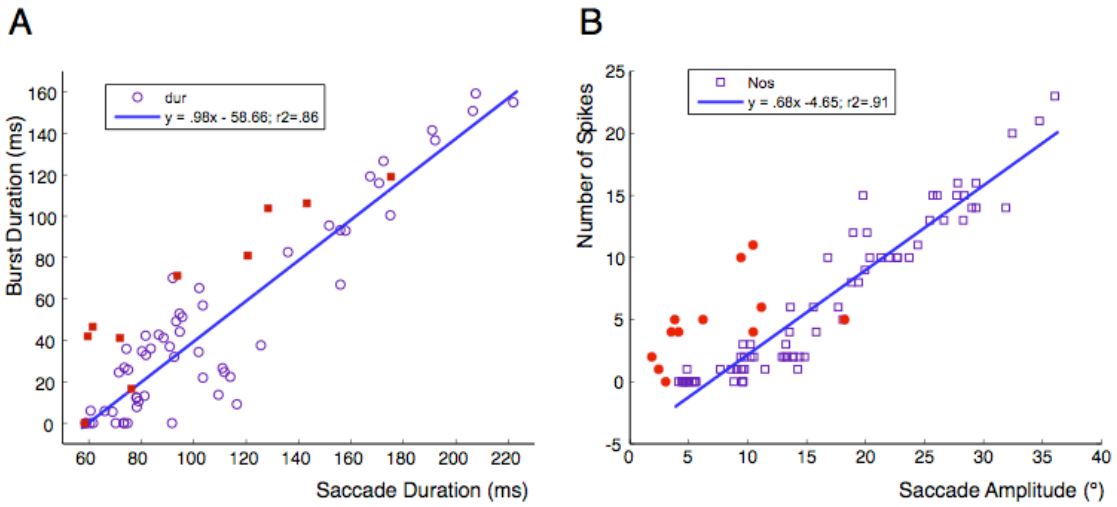

Figure 3. Relationship between burst neuron discharge and saccade metrics. A. Burst duration versus movement duration for visually elicited saccades (open blue circles) and electrically elicited fast phases (filled red squares). B. Number of spikes in the burst versus movement amplitude for visually elicited saccades (open blue squares) and electrically elicited fast phases (filled red circles).

It is unclear why there are different relationships between the burst or pause neuron activity and the rapid eye movements for natural versus electrically elicited movements. One possibility is that high rate synchronous electrical activation of a subset of afferent fibers fails to activate the fast phase brainstem circuitry that is also responsible for saccadic eye movements. However, it is also possible that the observed fast phase eye movements are smaller and shorter than those actually commanded by the brainstem burst generator because the synchronous vestibular input is overdriving the resetting fast phase eye movements with occult slow phases, producing longer pauses and bursts for a given duration fast phase, and more burst spikes for a given amplitude fast phase. Basically, the natural alternation of slow and fast phases may be disrupted by such electrical stimuli. This presents an interesting question for future study, and may have profound consequences for the efficacy of a vestibular prosthesis during prolonged stimulation.

2. We have now analyzed the resting discharge of a subset of our single vestibular neuron data to determine if there are differences in the coefficients of variation

(CV*) for neurons that are driven by electrical stimulation of the vestibular end organ versus neurons that are not driven electrically. It is well known that irregular vestibular afferents are more sensitive to galvanic stimulation than are regular vestibular afferents. These afferent fibers types tend to innervate hair cells in different regions the crista ampullaris. They have different endings on different hair cell types, and they have a different characteristic discharge in response to angular acceleration. Regular afferents tend to respond with a tonic discharge related to angular velocity whereas irregular afferents tend to have a phasic tonic discharge related to velocity and acceleration. Since we intend to tailor the electrical stimulation parameters to match the transfer function between rotational inputs and neural discharge in driven afferents, it is important to know the distribution of afferent types that are driven by a vestibular prosthesis. Unfortunately, there is only a weak correlation between afferent fiber type and the discharge regularity of secondary vestibular neurons. Still, we decided to look for differences between neurons that can be driven by electrical stimulation from any canal versus those that can not be driven. A histogram of the results from a sample of ¼ of our driven neurons and an equal number of non-driven neurons from the same electrode recording tracks is displayed in Figure 4, below. For this sample, the median CV* for non-driven neurons was .163, and the mean was .213. The median CV* for driven neurons was .218, and the mean was .541.

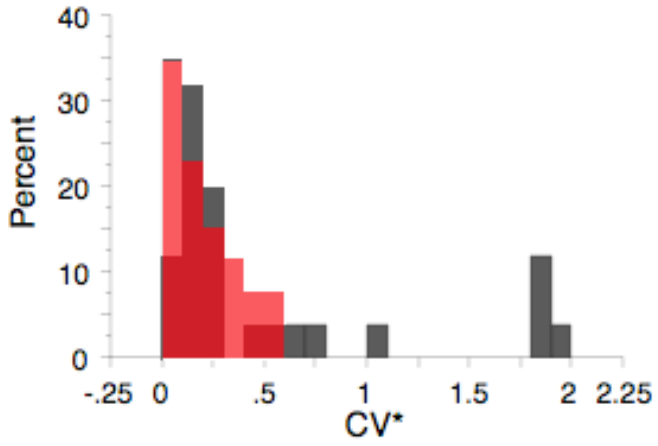

Figure 4. Coefficients of variation for vestibular nuclear neurons that are driven (black) or not driven (transparent red) by electrical stimulation from any implanted canal. The coefficients of variation are adjusted for resting rate (CV).*

To our great surprise, there appears to be a difference in CV* between driven and non-driven neurons recorded in the vestibular nucleus. Although this analysis is incomplete, it appears that driven neurons are more irregular in their discharge properties than are non-driven neurons. We do not yet know the resting discharge characteristics of the afferent fibers that drive these neurons, but this preliminary finding has inspired us to continue this analysis on the remaining neurons in our sample.

3. We have recorded single abducens neurons during high modulation frequency sine wave amplitude modulated stimulation. In the last quarter we noted that some

abducens neurons showed a sinusoidal modulation of firing rate in association with amplitude (current) modulated electrical stimulation driven at a constant frequency. This discharge was different from those of secondary vestibular neurons that we recorded, which display primarily recruitment and frequency following. This quarter we began to evaluate the discharge characteristics of such neurons during high modulation frequency stimulation, to see if at these higher frequencies the abducens motoneurons still mirrored the stimulus amplitude in the rate of their discharge. Figure 5 displays the discharge of a representative abducens neuron during 5 Hz sine wave modulated electrical stimulation at a fixed pulse frequency of 200 pps.

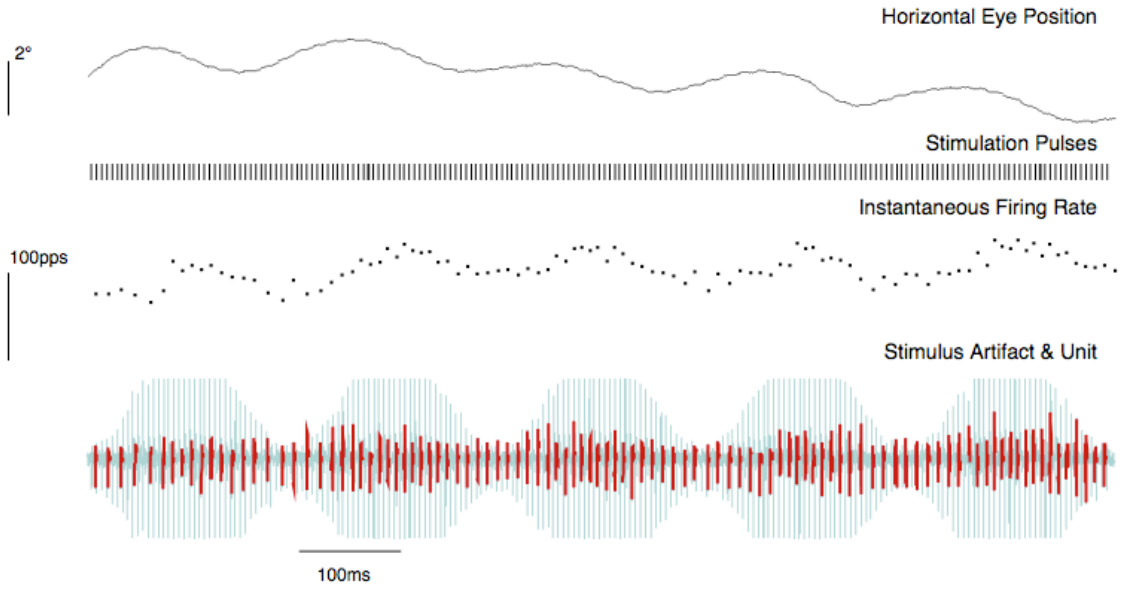

Figure 5. Left abducens neuron response to sine wave amplitude modulated electrical stimulation of the right lateral canal at 5 Hz, 200 pps, 100 µs per phase, 8 µs gap.

As can be seen in Figure 5, high modulation frequency sinusoidal AM electrical stimulation produces sinusoidal modulation of eye position and neuron firing rate, suggesting that amplitude modulation, even at high modulation frequencies, is expressed as a modulation of motoneuron firing rate. This convergence of serially recruited inputs appears to be an intrinsic property of the brainstem VOR circuitry, and is adequate to explain our behavioral observation across the normal range of operation of a vestibular prosthesis. The precise mechanism remains to be elucidated.

4. This quarter, we attempted to reduce afferent input into the vestibular nucleus with high, constant frequency electrical stimulation. Our hypothesis, derived from electrophysiological and psychometric studies in cochlear implant research, was that we could produce a low, stochastically determined, discharge in vestibular afferent fibers by driving them with trains of electrical stimuli that were well above their normal discharge frequency. The purpose of this would be to produce a reduction in resting discharge in an

overly active ear with electrical stimulation in that ear. Essentially, if this technique was successful, we could treat either irritative vestibular dysfunction, or loss of vestibular function, with electrical stimulation in the affected ear. The results of several such experiments in two animals are shown in Figure 6. In our initial experiments, each animal received electrical stimulation at 5000 pps for 2 seconds in the right lateral canal. We hypothesized that at low currents this stimulus would produce a right beating nystagmus that would grow in slow phase velocity with stimulation current. Such a response would be analogous to the response at lower, more physiological stimulation frequencies. However, with increasing current above an empirically determined point, the eye velocities would begin to decrease and ultimately, in theory, the slow phase eye velocity would reverse, as the stochastically determined rate of the afferent discharge in the stimulated vestibular nerve dropped below the normal resting rate, while the afferent fibers of the unstimulated contralateral vestibular nerve remained at their normal rate. It was further suspected that this process would have a time course within each stimulation trial, such that the initial stimulus pulses would produce higher slow phase velocities than the later stimulus pulses within each stimulation train.

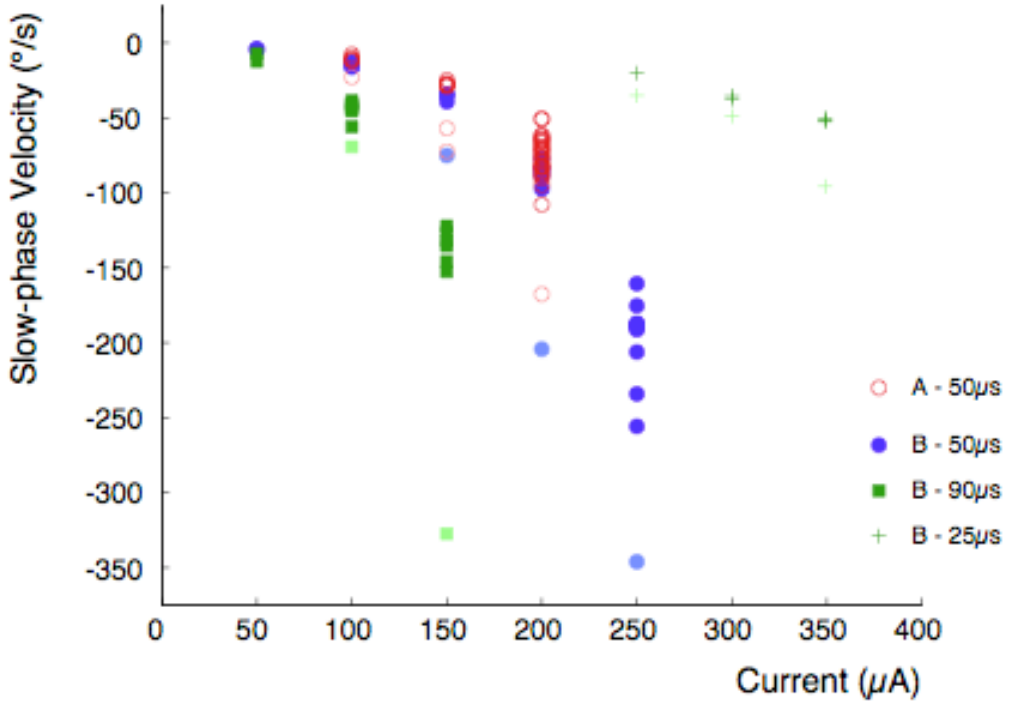

Figure 6: Slow phase velocity versus stimulation current at different phase durations for 2 s trains of 5K pps electrical stimulation of the right lateral canal in two monkeys (A and B). The average velocity of the first slow phase for each stimulus type is represented by the lightly shaded symbols of the same shape and hue.

The results displayed in Figure 6 suggest that our hypothesis may be incorrect. While the first slow phase always had a higher velocity than the later slow phases at each stimulation current, the result of increasing current until we reached the safe current limits, or observed current spread to the facial nerve, was a monotonic increase in slow phase velocity with current. There was no decrease in slow phase velocity or reversal of slow phase direction at the highest current levels.

As a result of experiments such as the one displayed in Figure 6, we hypothesized that we needed longer durations to produce the desired stochastic firing and the resulting changes in slow phase velocity. We conducted a second series of experiments with stimulation durations of 120 seconds. The result of one such experiment in monkey B from Figure 6 above, is displayed in Figure 7. The stimulation parameters are 5000 pps, 200 micro amps, 50 μs per phase, delivered to the right lateral canal electrode.

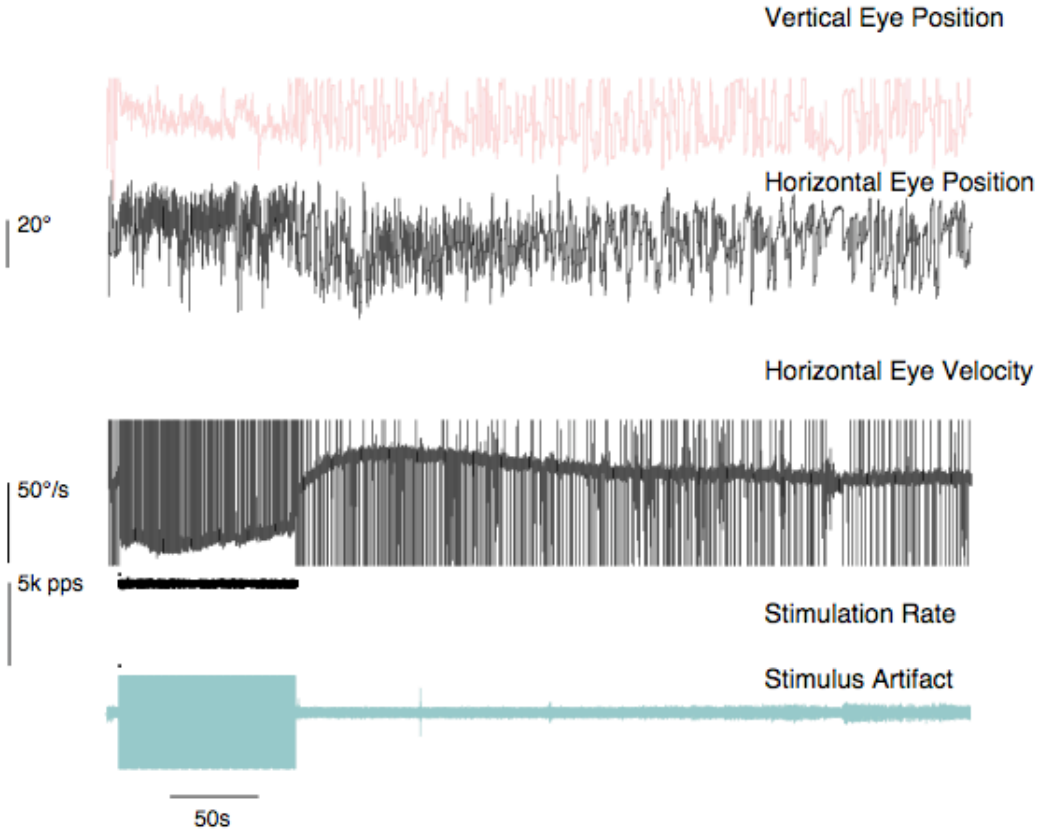

Figure 7. Slow phase eye movements resulting from 120 s of high frequency electrical stimulation of the right lateral canal.

The horizontal slow phase eye velocity displayed in Figure 7 reveals that the longer stimulation durations failed to produce a reversal of slow phase eye velocity during the period of electrical stimulation. The slow phase eye velocities were always to the left in response to right lateral canal stimulation. Following the stimulation there was a brief period of after-nystagmus followed by a prolonged period of reversed nystagmus (after-after nystagmus). The reversed nystagmus velocity decayed away with a relatively long

time course. Therefore, we currently have evidence of adaptation to very high frequency electrical stimulation, which is quite effective in driving slow phase eye movement. However, we have no evidence that we can induce low frequency stochastic firing in the vestibular afferents or produce a reversal of nystagmus direction during stimulation. We plan to continue our parameter exploration next quarter to make certain that we have not missed a critical stimulation parameter in our attempts to produce what would be a very useful response in the nerve and monkey behavior.

5. This quarter, we attempted to record from the vestibular nerve rootlets as they entered the brainstem in one of our monkeys. We only have a very small sample of such fibers currently, but we have obtained an interesting result. In previous quarters we showed that summation of rotational and electrical stimulation responses appeared to require the presence of separate independent channels for each stimulus type. This conclusion was driven by the observation that individual vestibular neurons could not represent the summation of electrical and rotational inputs in their discharge rates across the full range of electrical stimulation pulse rates and rotational frequencies for which we observed behavioral summation. However, we did not have clear evidence of such a separate channel because we had not recorded from the vestibular nerve.

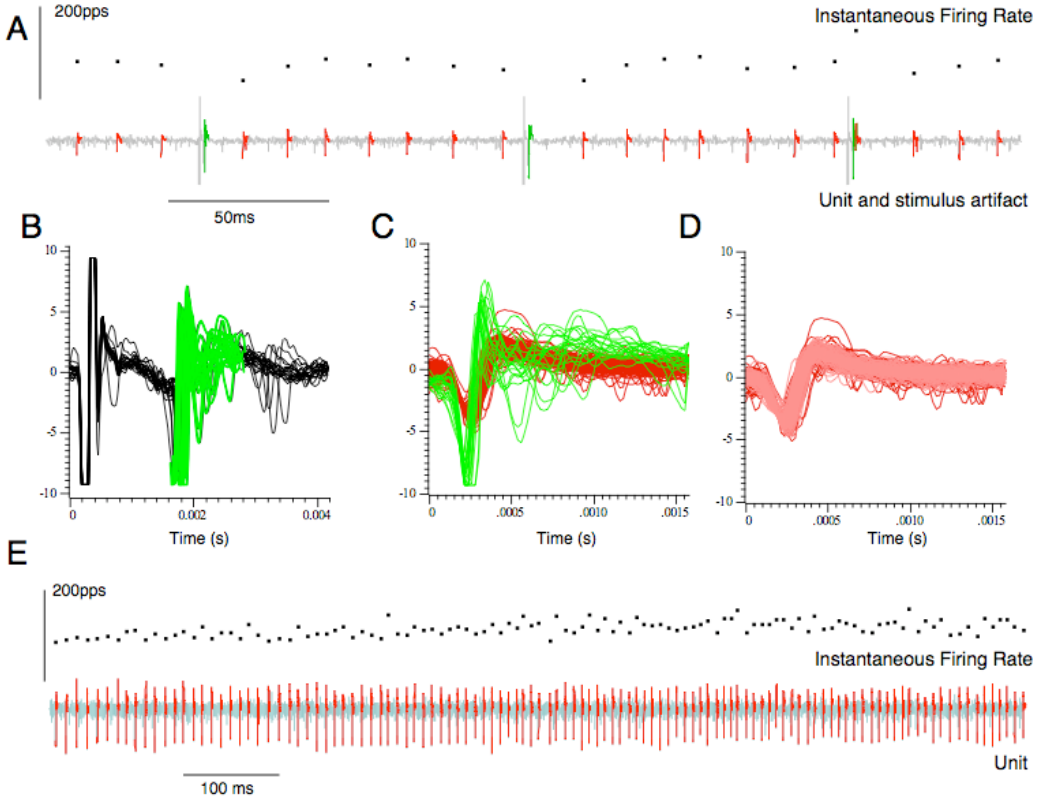

Figure 8: Simultaneous recording of a vestibular afferent fiber (green) and a vestibular nucleus neuron (red). A. Response of the two units during electrical stimulation (grey) of the lateral canal. B. Response of the afferent fiber aligned on the stimulation artifact. C. Aligned discharge of the afferent fiber and the adjacent neuron. D. Spontaneous discharge of the adjacent neuron (red) superimposed on the discharge during en-bloc rotation (pink). E. Spontaneous discharge of the adjacent neuron.

Figure 8 displays the response of a fiber and adjacent neurons simultaneously recorded in the medial vestibular nucleus.. In Figure 8A, the fiber (green) shows a spike discharge in close proximity to each electrical stimulus artifact (grey) resulting from electrical stimulation of the lateral canal. The adjacent neuron (red) is not driven by lateral canal stimulation, but fires spontaneously. In Figure 8B, the spike discharge of the afferent fiber is aligned on the electrical stimulation artifact (black). The discharge of the adjacent neuron is not consistently time-locked to the stimulation artifact, and therefore its unit spikes are not highlighted. Figure 8C shows the afferent fiber discharge superimposed on the discharge of the adjacent neuron, showing that these two units have different shapes and amplitudes. Figure 8E shows the spontaneous discharge of the adjacent vestibular nucleus neuron, but the discharge of the afferent fiber is absent. The afferent fiber is not spontaneously active. In Figure 8D, the spikes isolated during whole body rotation (pink) and those sorted within a stimulation train (red) are superimposed, which demonstrates that we recording from the same adjacent neuron.

Taken together, we see two channels of information represented in the simultaneous recording of an afferent fiber and an adjacent vestibular neuron. Many neurons in this area within the medial vestibular nucleus are modulated by rotational stimuli. Some are driven by electrical stimulation of the lateral canal or posterior canals, but many are not. Those neurons that are modulated by rotational stimulation but are not driven by electrical stimulation represent a channel sensitive to rotational stimulation alone. The afferent fiber, on the other hand, is driven by electrical stimulation, but is not spontaneously active and is not modulated during rotation. This fiber represents a channel sensitive to electrical stimulation alone. Summation of the inputs of these two channels at a later stage in the brainstem processing of combined rotational and electrical stimulation would produce the behavior that we have observed without requiring that the summation occur within individual secondary vestibular neurons. Since this fiber was not identified prior to electrical stimulation, we have begun to reexamine our multiple single unit recordings to determine if other fibers or somatic recordings display such discharge characteristics.

6. As of the end of Quarter 19, we have collected click-evoked auditory brainstem potentials (ABRs) in eight monkeys implanted with the UW/Cochlear vestibular prosthesis. Pre-operative ABRs have also been obtained in a ninth animal, scheduled for implantation in Quarter 20. A tenth animal was only implanted with a fine wire percutaneous electrode stimulation array and was canal plugged. For simplicity, the data for this animal are omitted from Table 1 below.

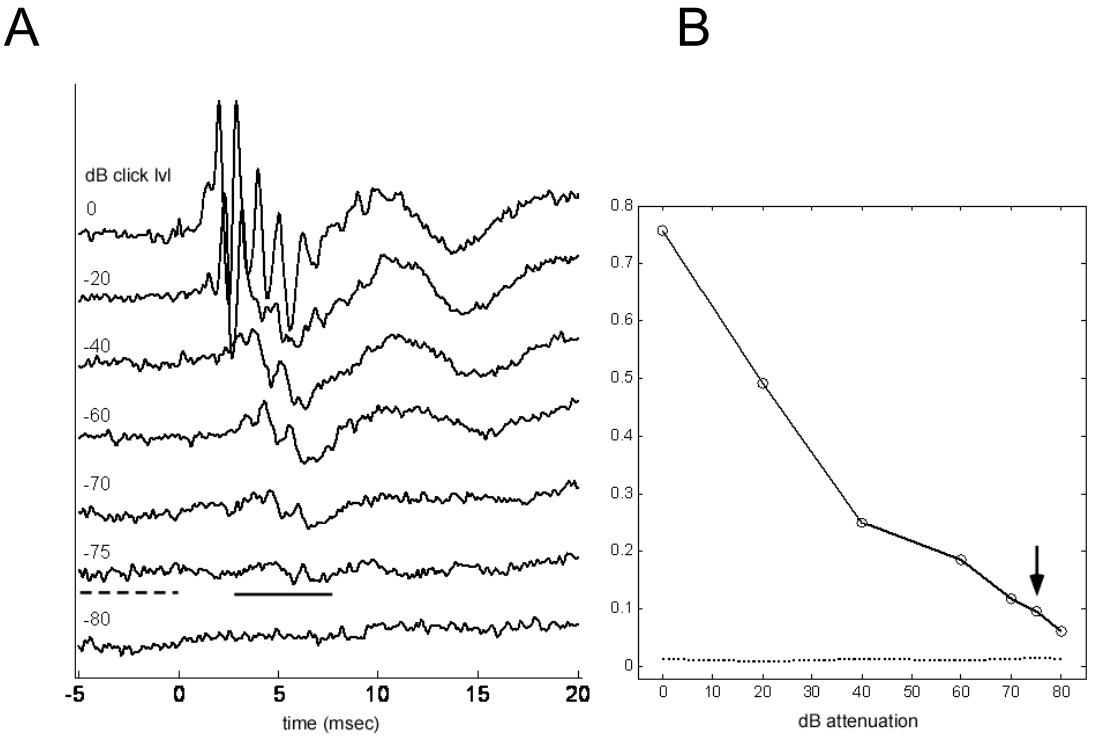

Figure 9. A) ABR series for the implanted right ear of Animal 6, 8 days after its second implantation surgery. Dashed and solid lines denote regions of noise and signal analysis, respectively, as described in the text. B) Waveform amplitude (solid line) and noise level (dashed line) as a function of stimulus attenuation for the waveforms in A. Arrow points to the estimated threshold level of -75 dB.

The example in Figure 9 illustrates the automated procedure that we now use to estimate response thresholds in preparation for a manuscript. Figure 9A displays a typical series of ABR recordings for the right ear of one animal, 8 days after vestibular prosthesis implantation in the right ear. Each trace is the average of 500 presentations of 100 μs acoustic clicks. The highest-intensity click (*top trace*) results in a clear multi-peaked waveform that decreases in amplitude and increases in latency as click intensity decreases until a waveform is no longer visible (*bottom trace*). We define threshold objectively as the minimum click intensity that produces an ABR waveform amplitude exceeding a criterion level defined by baseline recording noise. The detailed procedure is as follows: first, a baseline noise level is obtained for each trace by calculating its standard deviation over the 5 ms time segment preceding the click (*dashed horizontal bar*). Next, the largest peak-to-valley excursion (i.e. positive-to-negative) is found that occurs within a 5 ms time window following the click (*solid horizontal bar*); this signal window begins at 2.5 ms and is intended to encompass waves III-V of the ABR, which are generally the largest components at low stimulus levels. Finally, the peak-to-valley stimulus amplitude versus intensity function is interpolated to 1 dB steps, and the point where the function crosses 6 times the baseline noise level is defined as threshold. Figure 9B shows a graph of the interpolated function (*solid line*) and noise level (*dashed line*) for the data displayed in

Figure 9A. Threshold for this example occurs at -75 dB, as denoted by the vertical arrow.

Animal	# Surg.	Pre-surgery		Post-surgery		5+ months	
1 ‡	2			-73	-65	-80	-67
2 †	3			-63|	-55		
3 †	2&			-79	-36	-67	-41
4 †	2			-74	-5	-87	0
5 †	2			-76	-75		
6 *	2	-75	-71	-70	-75	-84	-87
7 *	1	-75	-77	-66	-62	-72	-76
8 *	1	-65	-71	-77	-35	--	--
9	0	-77	-85	--	--	--	--

Table 1. Summary of ABR thresholds for animals implanted with the Nucleus Freedom-based vestibular prosthesis. Thresholds are expressed as decibels with respect to the loudest click possible, so lower negative values correspond to higher click intensities. For each of the three time periods, the left and right columns list thresholds for the left (non-implanted) and right (implanted) ears, respectively. Grey blocks indicate unavailable data; blocks with "--" indicate data to be collected in the future. For Animal 1 (‡), the earliest post-surgery data was collected 14 months after the last surgery; for all other animals, the data was collected within 4 months (\|†) or 2 weeks (*) of the last surgery. Animal 3 (&) was implanted with an array of wire electrodes in its first surgery.

ABR thresholds for the eight monkeys that received the standard vestibular prosthesis and the single monkey to be implanted in Quarter 20 are shown in Table 1. Thresholds are expressed in decibels with respect to a non-attenuated click of ~110 dB SPL. Note that most of the implanted animals underwent multiple surgeries. For all but one animal, the "post-surgery" table values correspond to thresholds obtained within 4 months of the animal's last surgery; for the remaining animal (Animal 1), the values correspond to thresholds obtained more than a year after the last surgery because earlier data are not available. For 5 of 8 animals, the threshold in the right implanted ear was within 15 dB of the left non-implanted (control) ear. Mean thresholds for these five animals were -69.6 (+/- 5.2 std) and -66.4 dB (+/- 8.6) for the left and right ears, respectively. The other animals (3, 4 and 8) had comparable control thresholds of -76.7 dB (+/- 2.5), but the right ear thresholds ranged from -5 to -36 dB, suggesting a moderate to severe hearing loss related to implantation.

In several animals, thresholds were collected at least 5 months after the last implant surgery ("5+ months"). Thresholds generally improved for both the left and right ears. In Animal 4, however, the -5 dB right ear threshold increased to 0 dB even as the left ear threshold remained low, demonstrating that the severely compromised hearing in the implanted ear did not improve with time. Similarly, the right ear threshold of Animal 3 remained elevated beyond the 5-month mark.

In three animals, thresholds were obtained prior to the first implantation surgery, providing a "pre-surgery" control for both ears. For all three animals, thresholds in the non-implanted left ear, obtained within 2 weeks and after 5 months of the last surgery, remained within 12 dB of their pre-surgery values. Thresholds for the implanted ear fluctuated somewhat more across time periods, but in two animals the right ear thresholds after 5 months were at or below their pre-surgery values. In Animal 8, however, the right ear threshold was 36 dB higher after surgery. Therefore, the before-after threshold comparison in this animal gave qualitatively similar results to the left-right comparisons described above.

We conclude from this data that implantation of the UW/Cochlear vestibular prosthesis can be performed without compromising hearing in our monkeys. In 5 of 8 monkeys, there was minimal post surgical hearing loss in the implanted ear. In two monkeys, implantation produced moderate hearing loss. This recovered somewhat with time in one monkey. We do not have the long-term data for the other animal. In one monkey, there was severe hearing loss in the implanted ear.

7. We have presented our results in scientific meetings during this quarter. The presentation titles and authors are listed below.

Jay Rubinstein; James Phillips; Kaibao Nie; Leo Ling; Steven Bierer; Elyse Jameson; Trey Oxford; Clinical, Scientific and Regulatory Roadmap for a Human Vestibular Implant, Association for Research in Otolaryngology Midwinter Meeting, 2011

James Phillips; Leo Ling; Steven Bierer; Albert Fuchs; Chris Kaneko; Trey Oxford; Kaibao Nie; Amy Nowack; Jay Rubinstein; Use of Single Unit Recording to Understand the Neural Mechanism of a Vestibular Implant, Association for Research in Otolaryngology Midwinter Meeting, 2011

Jay Rubinstein, Update on First Human Trial of Vestibular Implant, Colorado Audiology-Otology Conference, Vail, CO, 2011

Jay Rubinstein, First Results with a Human Vestibular Implant, Holy Hour Speaker, Dept ExpORL, Katholieke Universiteit Leuven, Belgium, 2011

James Phillips, Steven Bierer, Leo Ling, Jay Rubinstein, Shawn Newlands, Amy Nowack, Kaibao Nie, Albert Fuchs, Chris Kaneko Comparison of monkey and human responses to electrical stimulation with a vestibular prosthesis. Neural Control of Movement Meeting, 2011

8. We have submitted two abstracts and a paper during this quarter. The titles and authors are listed below.

Jay Rubinstein, Feasibility studies of the UW/Nucleus vestibular implant for Meniere's disease: First Human Data, Collegium ORL, accepted to be presented October 5, 2011 in Bruges, Belgium

L Ling, S Bierer, A.F. Fuchs, C.R.S. Kaneko, S.D. Newlands, K Nie, A Nowack, J.T. Rubinstein, J.O. Phillips Transient and sustained components in response to electrical stimulation of vestibular end organ. Society for Neuroscience Abstract, Neurosciences 2011

James O. Phillips, Steven M. Bierer, Leo Ling, Kaibao Nie, and Jay T. Rubinstein, Real time communication of head velocity and acceleration for an externally mounted vestibular prosthesis. IEEE Engineering in Medicine and Biology Society, submitted

Objectives for Quarter 20

1. In the next quarter we will record additional brainstem neurons during electrical stimulation. We will look in particular at several unit types that have been mapped within the chambers of our existing monkeys.

a. We will record from neurons in the brainstem burst generator, including short lead burst and omnipause neurons. We will compare their discharge during active gaze shifts and combined head rotation when the gaze shifts are normally occurring versus when they are interrupted with brief trains of electrical stimulation of the vestibular end organ in the plane of the canal aligned with the gaze shift. Our objective will be to determine if the changes in gaze velocity that we have previously observed with electrical stimulation, are due to vestibular signals passing through the saccadic burst generator or are due to direct vestibulo-ocular reflex input to motoneurons.

b. We will continue to record from vestibular nucleus neurons during amplitude modulated electrical stimulation, with special attention to neurons driven at multisynaptic latency in the medial vestibular nucleus. Such neurons, or neurons in the neighboring nucleus prepositus, may provide the intermediate step in the conversion of recruitment based coding scheme in the secondary vestibular neurons, to the frequency based coding that we see in abducens neurons under these conditions.

c. We will continue to expand our very small sample of vestibular afferent fibers to understand the coding that takes place in the nerve and to characterize the coefficient of variation in these fibers. We have one monkey that will receive a chamber placed to record afferent fibers in Quarter 20. We hope to resolve the issue of whether we are primarily activating only irregular fibers with our stimulation, and whether we see some fiber activity that is only present during electrical stimulation.

d. We will record from abducens neurons during amplitude modulated constant rate electrical stimulation and during naturally elicited movements to see if the relationships between discharge frequency, eye position, and eye velocity remain the same in both conditions.

2. We will continue our behavioral recording, and continue to expand our longitudinal dataset contrasting vestibulo-ocular reflex response properties with the efficacy of electrical stimulation in the same canal planes.

3. We anticipate obtaining additional data from our one implanted human subject, and also obtaining data from a second subject. We will expand our dataset so that the

stimulation parameters used in humans match the range of parameters used during the non-human primate studies.

4. We will record behavioral and unit data from intratympanic gentamicin lesioned monkeys during prolonged electrical stimulation with a vestibular prosthesis. We will contrast the electrically elicited eye movements and unit discharge recorded in animals with unilateral and bilateral vestibular lesions, and with intact vestibular function.